

Theory of substitutional and interstitial 3d impurities in silicon

Alex Zunger

Solar Energy Research Institute, Golden, Colorado 80401

U. Lindefelt

Department of Theoretical Physics, University of Lund, Sölvegatan 14A, S-223 62, Lund, Sweden

(Received 29 July 1982)

The chemical regularities in the electronic structure of substitutional and interstitial 3d impurities in silicon are studied through a self-consistent local-density-functional Green's-function calculation.

Despite 25 years of basic and applied research on the properties of transition atom (TA) impurities in semiconductors, they have been subjected only recently to theoretical studies.^{1,2} In this Communication we report the first theoretical study of the electronic properties of all tetrahedral substitutional (*S*) and interstitial (*I*) 3d impurities in an infinite host semiconductor. We use the recently developed³ first-principles quasiband crystal-field Green's-function method within the local density formulation of interelectronic interactions. The calculation is fully self-consistent, uses *ab initio* nonlocal pseudopotentials,³ avoids any spherical approximations to the potential or finite cluster models, and assumes an unrelaxed lattice. It reflects to within an excellent approximation (~ 0.1 eV in energies and 2–3% in charge densities) the predictions of the physical input, not computational approximations. We describe the chemical trends and the unifying physical principles underlying the diversity of phenomena in this system.

Figure 1 displays the variations in the impurity-induced gap energy levels for *S* and *I* impurities in silicon. The overall trends in these energies agree with previous cluster calculations.^{1,2} The results show four notable features. First, the *e* level is below the t_2 level for *S* impurities, whereas the order is reversed for *I* impurities (as predicted by the point-ion model and cluster calculations^{1,2}). Second, the *e*- t_2 crystal-field splitting for *S* impurities is 1.5–3 times larger than for *I* impurities, reflecting the stronger and more anisotropic crystal-field potential at the *S* site. The splitting for *I* impurities is about 5 times larger than that calculated in the spherical potential (muffin-tin) cluster approximation.² Third, the model predicts a number of simple chemical trends in the system's electrical activity with the site location of the impurity. For example, whereas an isolated Cu impurity is predicted to be electrically inactive in an *I* site (with filled t^6e^4 shells), it is predicted (and found⁴) to be electrically active as a triple acceptor t^3e^4 when displaced into an *S* site.

The model also predicts the light *I* impurities (V, Cr, Mn) are capable of both donating and accepting carriers due to their partially occupied *e* and t_2 levels, whereas, the heavy *I* impurities (Ni, Cu) are predicted to be mostly inactive (if they do not cluster or precipitate⁵). This may explain the long-known empirical fact (e.g. Ref. 5) that even minute contaminations of silicon by light TA impurities (Ti, V) considerably shorten the lifetime of all free carriers (leading to vanishing silicon solar cell efficiencies), whereas even a 1000 times larger contamination by heavy TA impurities (e.g., Cu) can be tolerated with no effect. Fourth, the calculation predicts a number of switch-on (switch-off) thresholds for the appearance (disap-

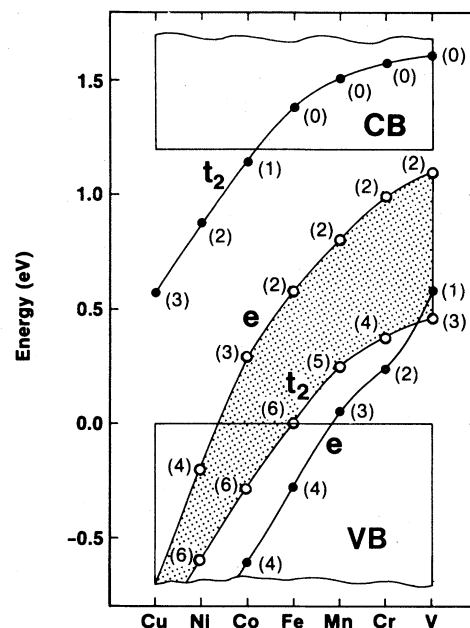


FIG. 1. Variations in the gap energy levels for neutral *S* (solid circles) and *I* (open circles) impurities in silicon. Numbers in parentheses indicate level occupations used; the shaded area denotes the crystal-field splitting for *I* impurities.

pearance) of neutral defect levels in the band gap as a function of the impurity valence Z . Progressing from heavy to light impurities, the S e level first appears past Mn, and the I e level appears past Co, the I t_2 level appears past Fe, and the S t_2 level disappears past Co.

Figure 2 shows how the electronic charge is radially distributed around the impurity site (at the origin) for Fe in a S or I site in silicon. It depicts the total electronic charge $Q_D(R) = \int_0^R \rho_D(\vec{r}) d\vec{r}$ contained in a sphere of radius R in the defect (D) containing system, the charge $Q_H(R) = \int_0^R \rho_H(\vec{r}) d\vec{r}$ of the pure host (H) crystal, and their difference $Q = Q_D - Q_H$, corresponding to the effective electronic charge of a bonded impurity atom. Here, $\rho_D(\vec{r})$ and $\rho_H(\vec{r})$ denote the self-consistent charge density of the defect and host crystals, respectively. Figure 2 shows that both S and I impurities attain charge neutrality [$Q(R_{\text{pert}}) = \Delta Z$, where $\Delta Z = Z_D - Z_H = 4$ for S iron and $\Delta Z = Z_D = 8$ for I iron] already inside the central cell (having in Si a nearest-neighbor radius of 4.44 a.u.). The calculation defines a characteristic radius R_{pert} outside which the impurity-induced perturbation vanishes. It further provides a natural theoretical definition of an effective atomic radius for a tetrahedrally bonded TA, simply from $Q_D(R) = Z_D$, i.e., the radius enclosing a charge equivalent to the nominal valence. This yields, for example, $R_I = 2.65$ a.u. and $R_S = 2.50$ a.u. for the I and S sites of Fe, respectively (Fig. 2), which is remarkably close to the empirical, site-independent Slater-Bragg⁶ tetrahedral radius of the Fe atom (2.64 a.u.). The quantum-mechanical calculation produces more refined radii ($R_I = 2.60, 2.62, 2.65, 2.66, 2.68$, and 2.72 a.u. for Ni, Co, Fe, Mn, Cr, and V, respectively, exhibiting an increase in atomic size with decreasing valence) that are nevertheless closely tracked by the classical radii.⁶ Our calculation further shows that the net impurity ionic charge (the amount by

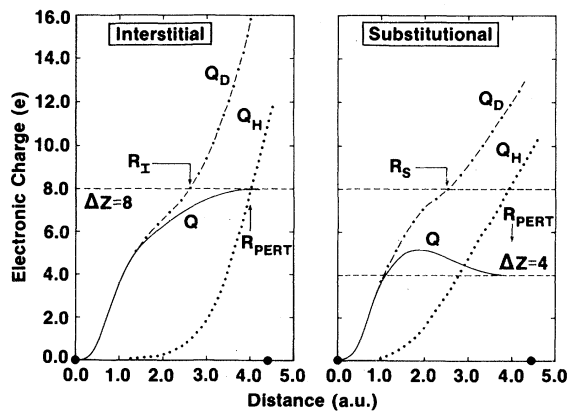


FIG. 2. The defect Q_D , host Q_H , and impurity Q charges in a sphere of radius R around the I and S iron impurities in silicon.

which the positive core charge ΔZ exceeds the electronic charge inside the perturbation radius) closely follows the phenomenological host-impurity electronegativity difference $\Delta\chi$. At the central-cell boundary, we find a positive net charge of $\leq 0.03e$ for Ni, Co, and Fe with $\Delta\chi = 0$ on Pauling's scale, whereas for Mn, Cr, V, and Ti we find a net charge of 0.12, 0.07, 0.08, and 0.13 e , respectively, following the trends in the electronegativity differences of 0.3, 0.2, and 0.2, and 0.3. The results suggest that ionic charge transfer is relatively unimportant to these systems. The chemical trends evident in Fig. 1 further suggest that isolated electropositive impurities (e.g., rare-earth elements, $\Delta\chi > 0.6$) are likely to have no deep traps in silicon.

The significance of the screening mechanisms leading to the confinement of the impurity charge Q in the central cell (Fig. 2) can be appreciated by decomposing Q into contributions of different quantum states. We partition Q into a gap contribution

$$Q_{\text{gap}}(R) = \sum_i^{N_i} \int_0^R |\psi_i|^2 d\vec{r}$$

arising from the impurity-induced gap wave functions ψ_i with occupation numbers N_i (numbers shown in parentheses in Fig. 1), and into a contribution $\Delta Q_{\text{VB}}(R)$ arising from the displaced valence-band (VB) charge (calculated as $Q_D^{\text{VB}} - Q_H$, where Q_D^{VB} is the portion of Q_D arising from the perturbed valence-band states alone). ΔQ_{VB} constitutes the self-consistent screening response of the host to the bare impurity perturbation (difference between the impurity and host ionic pseudopotentials). The results are shown in Fig. 3 and as expected, at a large distance from the impurity, the electrons occupying the gap levels produce all of the impurity atomic charge Q [$Q(\infty) = Q_{\text{gap}}(\infty) = \Delta Z$], whereas the valence band resumes its unperturbed density [$\Delta Q_{\text{VB}}(\infty) = 0$]. Remarkably, however, the impurity attains the charge neutrality limit $Q(R) = \Delta Z$ already at a radius $R \cong 3-5$ a.u., where the gap electrons contribute only 50% (I) to 75% (S) of Q . Figure 3 shows how the difference is made up by a rearrangement of the VB charge (shaded area denoting ΔQ_{VB}). As a result of an effective displacement of VB charge into the central cell, the system achieves local charge neutrality already at the cell boundary despite the rather extended nature of the gap wave functions. Figure 3 also shows the distinguishing features of S impurities. Their gap charge Q_{gap} tracks the impurity charge Q considerably more closely than in the I case. Also, the polarizing displacement of the VB charge occurs in the S case on a significantly shorter distance scale. For comparison, recall that free atoms show a perfect tracking $Q(R) \equiv Q_{\text{gap}}(R)$ (all electrons contribute to the atomic charge), and that shallow impurities (e.g., Si:P) manifest a very slow tracking⁷ ($Q_{\text{gap}} \ll Q$ in the central cell). Finally, the impurity charge Q in the S case shows a pronounced max-

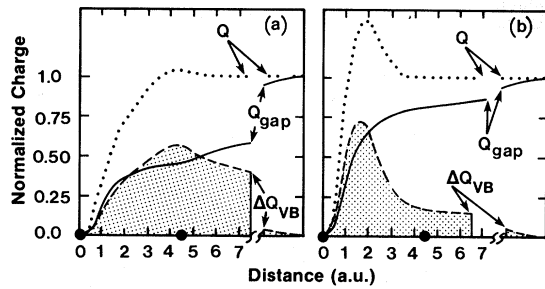


FIG. 3. Decomposition of the radial impurity charge Q into the gap contribution Q_{gap} and the valence-band contribution ΔQ_{VB} for (a) I and (b) S neutral Si:Mn. The charge is normalized to its asymptotic value ΔZ .

imum (which overshoots the asymptotic limit ΔZ) arising from the formation of strong bonding resonances that are absent in the weakly interacting I case.

The efficient screening of S impurities manifested by the short wavelength of the displaced VB charge also explains the remarkable stabilization in the narrow band gap of many energy levels corresponding to different ionized states.⁸ Figure 4 compares $Q_{\text{gap}}(R)$ and $\Delta Q_{\text{VB}}(R)$ for neutral (A^0 with occupation e^3) and negatively charged (A^- with occupation e^4) substitutional Si:Mn. It shows that, whereas $Q_{\text{gap}}(R)$ increases as an electron is added into the gap level, $\Delta Q_{\text{VB}}(R)$ shows a compensating decrease. Much like a pool below a waterfall, the VB resonances rearrange in response to adding charge to the gap level so that VB charge leaks out of the central cell. We find that this remarkable self-regulating behavior, first envisioned by Haldane and Anderson,⁸ leads to a nearly neutral central cell ($Q_{\text{gap}} + \Delta Q_{\text{VB}} \approx \Delta Z$ in Fig. 4) even for impurities with a nonzero formal charge. It enables, therefore, different charged states to have similar energy levels, in sharp contrast to free TA. This phenomena has the potential of explaining the pinning of gap levels, which leads to the formation of Schottky barriers in metal-semiconductor systems.

We find that the efficient screening of the Coulomb interactions leads to a substantial reduction in the intra-atomic repulsion energy U_d : a total energy calculation of the $A^0 + e \rightarrow A^-$ process⁹ produced $U_d = 0.18$ eV, which is more than two orders of magnitude lower than the free-atom value for Mn. This dramatic reduction in the correlation energy suggests that a significant rearrangement of the free-atom orbital configuration s^nd^m may occur in the solid. We calculated the effective orbital configuration of a TA in silicon. First, Fig. 5 shows a partial-wave decomposition of the defect charge $Q_D(R) = \sum_l Q_{Dl}(R)$ for all S and I impurities (taken at the central-cell radius). Whereas all the non- d content of the central cell is seen to be small and nearly constant, the d content is both large and decreases rapidly with ΔZ . Second, to construct a simple model for the effective

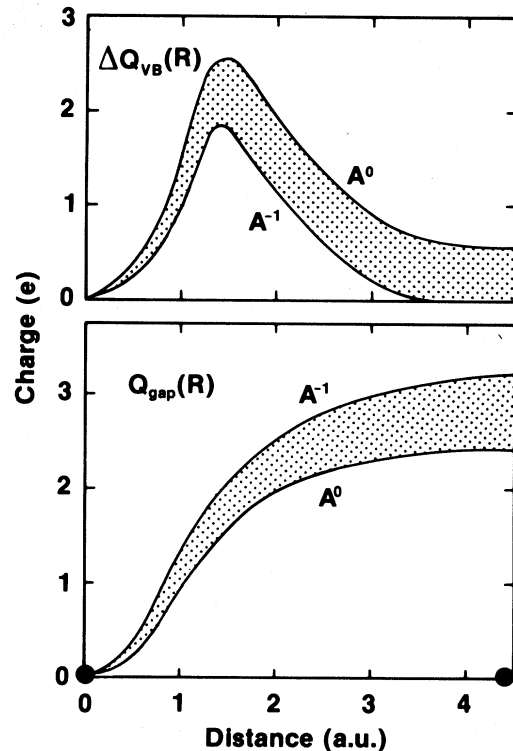


FIG. 4. Radial variations in the gap and valence-band contributions to the impurity charge for neutral (A^0) and negatively charged (A^-) substitutional Si:Mn. Shaded area denotes the charge redistribution upon charging A^0 .

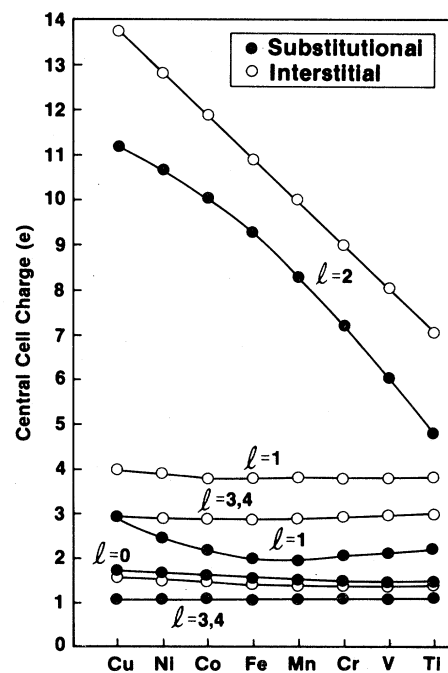


FIG. 5. Partial-wave analysis of the central-cell charge Q_D for S and I impurities in silicon.

configuration of the impurity atom in the solid, one has to subtract the impurity-independent background contribution of the host states penetrating the central cell from Q_{ID} . We subtract the l -decomposed host charge $Q_{IH}(R)$ for I impurities, and the l -decomposed vacancy charge³ $Q_{IV}(R)$ for S impurities. This defines effective orbital configurations $Q_{ID} - Q_{IH}$ and $Q_{ID} - Q_{IV}$ of "isolated" I and S impurity atoms, respectively, renormalized by their self-consistent interactions with the crystal. We find that (Fig. 5) *whenever the d shell can accommodate more than its electrons (TA lighter than Cu) the s electrons are promoted into the d shell, leading to an $\approx d^{n+m}$ configuration.* In contrast to free atoms, the energy cost of this process is likely to be small due to the substantial reduction of U_d in the solid. Our results confirm the classical hypothesis of Woodbury and Ludwig,¹⁰ suggesting an $s \rightarrow d$ promotion for I impurities, but con-

tradict their assumption of a reversed $d \rightarrow sp$ promotion for S impurities.

Our predicted s - d population inversion further suggests a simple explanation to the diffusion puzzle¹¹: whereas Ni is known to be an extremely fast I diffuser in Si (diffusion constant $D \sim 10^{-4}$ cm²/s, typical of liquids), the lighter TA, like Ti, are extremely immobile in silicon ($D \sim 10^{-8} - 10^{-10}$ cm²/s). We suggest that this is so because Ni has an effective noble-atom-like closed-shell configuration $\approx d^{10}$ in silicon and is therefore both small and chemically passive. On the other hand, Ti and V exist in silicon as open-shell species with large perturbation radii and hence have a far greater propensity for both steric and chemical interactions with the host.

We are grateful to the staff of the SERI computer center for their assistance.

¹L. A. Hemstreet, Phys. Rev. B **15**, 834 (1977).

²G. G. DeLeo, G. D. Watkins, and W. B. Fowler, Phys. Rev. B **23**, 1851 (1981); **25**, 4962, 4972 (1982).

³U. Lindefelt and A. Zunger, Phys. Rev. B **24**, 5913 (1981); **26**, 846 (1982).

⁴R. N. Hall and J. H. Racette, J. Appl. Phys. **35**, 379 (1964).

⁵R. H. Hopkins, R. G. Seidensticker, J. R. Davis, P. Rai-Chaudhury, and P. D. Blais, J. Cryst. Growth **42**, 493 (1977).

⁶J. C. Slater, *Symmetry and Energy Bands in Crystals* (Dover, New York, 1972), p. 55.

⁷G. Kirczenow, R. Barrie, and B. Bergersen, Phys. Rev. B **19**, 2139 (1979).

⁸F. D. M. Haldane and P. W. Anderson, Phys. Rev. B **13**, 2553 (1976).

⁹A. Zunger and U. Lindefelt, Phys. Rev. B (in press).

¹⁰H. H. Woodbury and G. W. Ludwig, Phys. Rev. **117**, 102 (1960).

¹¹K. Graff and H. Pieper, *Semiconductor Silicon 1981* (Electrochemical Society, Pennington, N.J., 1981), Vol. 81-85, p. 331.